AMERICAN SOCIETY FOR MICROBIOLOGY | Antimicrobial Agents and Chemotherapy®

ANTIVIRAL AGENTS

In Vitro Evaluation of the Drug Interaction Potential of Doravirine

Kelly Bleasby,[a] Kerry L. Fillgrove,[a] Robert Houle,[a] Bing Lu,[a] Jairam Palamanda,[a] Deborah J. Newton,[a] Meihong Lin,[a] Grace Hoyee Chan,[a] Rosa I. Sanchez[a]

[a]Merck & Co., Inc., Kenilworth, New Jersey, USA

ABSTRACT Doravirine is a novel nonnucleoside reverse transcriptase inhibitor for the treatment of human immunodeficiency virus type 1 infection. *In vitro* studies were conducted to assess the potential for drug interactions with doravirine via major drug-metabolizing enzymes and transporters. Kinetic studies confirmed that cytochrome P450 3A (CYP3A) plays a major role in the metabolism of doravirine, with ~20-fold-higher catalytic efficiency for CYP3A4 versus CYP3A5. Doravirine was not a substrate of breast cancer resistance protein (BCRP) and likely not a substrate of organic anion transporting polypeptide 1B1 (OATP1B1) or OATP1B3. Doravirine was not a reversible inhibitor of major CYP enzymes (CYP1A2, -2B6, -2C8, -2C9, -2C19, -2D6, and -3A4) or of UGT1A1, nor was it a time-dependent inhibitor of CYP3A4. No induction of CYP1A2 or -2B6 was observed in cultured human hepatocytes; small increases in CYP3A4 mRNA (≤20%) were reported at doravirine concentrations of ≥10 μM but with no corresponding increase in enzyme activity. *In vitro* transport studies indicated a low potential for interactions with substrates of BCRP, P-glycoprotein, OATP1B1 and OATP1B3, the bile salt extrusion pump (BSEP), organic anion transporter 1 (OAT1) and OAT3, organic cation transporter 2 (OCT2), and multidrug and toxin extrusion 1 (MATE1) and MATE2K proteins. In summary, these *in vitro* findings indicate that CYP3A4 and CYP3A5 mediate the metabolism of doravirine, although with different catalytic efficiencies. Clinical trials reported elsewhere confirm that doravirine is subject to drug-drug interactions (DDIs) via CYP3A inhibitors and inducers, but they support the notion that DDIs (either direction) are unlikely via other major drug-metabolizing enzymes and transporters.

KEYWORDS doravirine, HIV, drug interactions

Human immunodeficiency virus (HIV) treatment has improved significantly since the first therapies emerged in the 1980s. Current drug regimens offer patients durability and improved convenience so that HIV is now a chronic, rather than a life-threatening, disease. The life expectancy of people living with HIV has dramatically increased: for example, life expectancy at age 20 for individuals with HIV living in California in 2011 has been estimated at 53 years (1). As the life expectancy of people living with HIV increases, so will the number who, in addition to carrying HIV, develop age-related comorbidities, such as diabetes (2, 3). In the case of people living with HIV, these comorbidities are more prevalent and can occur at a younger age than in the general population (2, 3). Polypharmacy, in the aging HIV population, leads to an increased risk for drug-drug interactions. The aims of development of new therapies include reducing adverse effects and undesirable drug interactions, and increasing convenience and ease of administration, while maintaining efficacy.

Doravirine is a novel nonnucleoside reverse transcriptase inhibitor designed to overcome the limitations of other drugs in the class. It is administered in combination with other antiretroviral agents or as a three-drug single-tablet regimen with lamivu-

Citation Bleasby K, Fillgrove KL, Houle R, Lu B, Palamanda J, Newton DJ, Lin M, Chan GH, Sanchez RI. 2019. *In vitro* evaluation of the drug interaction potential of doravirine. Antimicrob Agents Chemother 63:e02492-18. https://doi.org/10.1128/AAC.02492-18.

Address correspondence to Rosa I. Sanchez, rosa_sanchez@merck.com.

Received 28 November 2018
Returned for modification 28 December 2018
Accepted 31 January 2019
Accepted manuscript posted online 11 February 2019
Published 27 March 2019

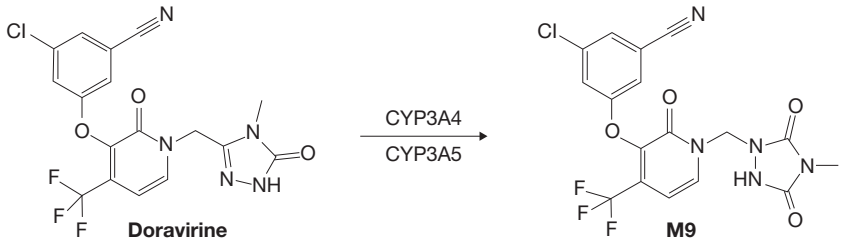

FIG 1 Cytochrome P450 (CYP)-mediated oxidation of doravirine to metabolite M9.

dine and tenofovir disoproxil fumarate (TDF) (4, 5). *In vitro*, doravirine has similar activity against HIV-1 wild-type virus and the K103N, Y181C, and K103N/Y181C mutants (6). Previously reported results showed that doravirine is metabolized primarily to an oxidative metabolite, M9, by cytochrome P450 3A4 (CYP3A4) and, to a lesser extent, by CYP3A5 (Fig. 1) (7). Doravirine showed moderate binding to human plasma proteins, good passive permeability *in vitro*, and low clearance following intravenous administration (7). Although doravirine is a P-glycoprotein (P-gp) substrate, data from an absorption, distribution, and elimination study indicate that P-gp is not likely to play a significant role in the absorption or elimination of doravirine (7). In a phase 3 trial comparing doravirine-lamivudine-TDF with efavirenz-emtricitabine-TDF, the efficacy of doravirine-lamivudine-TDF at week 48 was noninferior to that of efavirenz-emtricitabine-TDF in antiretroviral therapy-naive adults with HIV-1 (8). In a second phase 3 trial in antiretroviral therapy-naive adults with HIV-1, the antiretroviral efficacy of doravirine was noninferior to that of ritonavir-boosted darunavir, both combined with two nucleoside reverse transcriptase inhibitors (9). In both trials, the combination with doravirine was generally safe and well tolerated.

This paper reports the results of *in vitro* studies to assess the potential for drug interactions with doravirine via major drug-metabolizing enzymes and with transporters known to be involved in clinically relevant drug interactions, including CYP enzymes and UDP-glucuronosyltransferase 1A1 (UGT1A1), the efflux transporters breast cancer resistance protein (BCRP) and P-gp, the hepatic uptake transporters organic anion transporting polypeptide 1B1 (OATP1B1) and OATP1B3, the bile salt extrusion pump (BSEP), the renal uptake transporters organic anion transporter 1 (OAT1) and OAT3, organic cation transporter 2 (OCT2), and the efflux transporters multidrug and toxin extrusion protein 1 (MATE1) and MATE2K (10, 11).

RESULTS

Kinetic characterization of CYP3A4- and CYP3A5-catalyzed oxidation of doravirine. The enzyme kinetics for recombinant CYP3A4 (rCYP3A4)- and rCYP3A5-catalyzed formation of metabolite M9 were determined under linear velocity conditions, and the resulting plots of velocity versus substrate concentration for rCYP3A4 and rCYP3A5 are shown in Fig. 2A and B, respectively; these data enabled the determination of the mean apparent Michaelis-Menten constant ($K_{m,app}$) values. The unbound fractions of doravirine in microsomal rCYP3A4 and rCYP3A5, at the protein concentration used for the kinetic studies, were 0.92 and 0.42, respectively; binding was not concentration dependent over the 0.5 to 5.0 μM doravirine concentration range for either enzyme. Correcting $K_{m,app}$ values for microsomal binding, the resulting Michaelis-Menten constant (K_m) values were 20.9 μM for rCYP3A4 and 31.1 μM for rCYP3A5, with mean maximum velocity (V_{max}) values of 2.3 and 0.15 pmol/min/pmol CYP, respectively. The intrinsic clearance (CL_{int}) values calculated from the Michaelis-Menten-derived K_m and V_{max} values were 0.11 μl/min/pmol CYP for rCYP3A4 and 0.0048 μl/min/pmol CYP for rCYP3A5.

Drug transporters involved in the disposition of doravirine. (i) Efflux of doravirine by BCRP. Bidirectional transport of [^{3}H]doravirine was measured across Madin-Darby canine kidney II (MDCKII) cell monolayers and MDCKII cell monolayers expressing

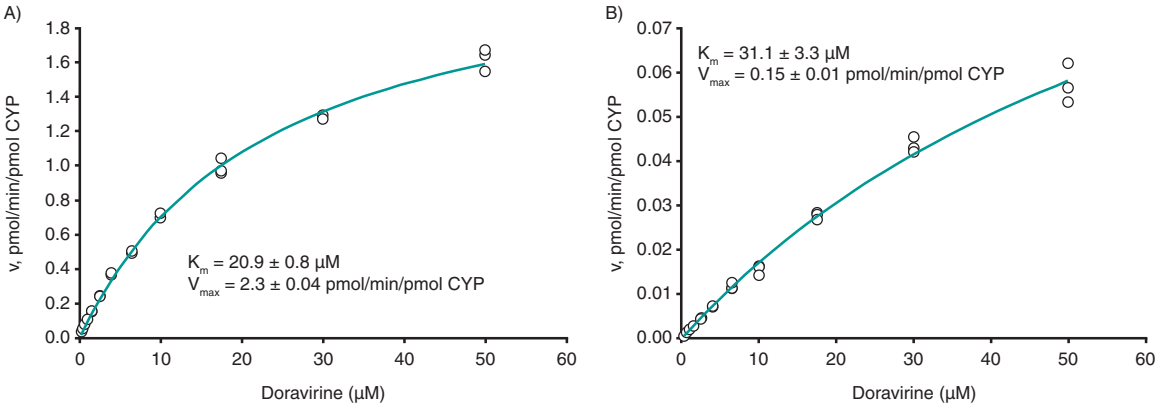

FIG 2 Velocity versus substrate concentration plots for rCYP3A4-catalyzed (A) and rCYP3A5-catalyzed (B) formation of M9 from doravirine. K_m, Michaelis-Menten constant; rCYP3A4/5, recombinant CYP3A4/5; V_{max}, maximum velocity.

BCRP (MDCKII-BCRP). The diffusion rate of doravirine across control MDCKII cell monolayers was moderate, with an apparent permeability (P_{app}) of 10.4 $\times$ 10^{-6} to 11.5 $\times$ 10^{-6} cm/s, while the positive control, prazosin, had a P_{app} of 22.7 $\times$ 10^{-6} cm/s (Table 1). The ratio of P_{app} from basolateral-to-apical divided by the P_{app} from apical-to-basolateral (B-A/A-B) of doravirine was 1.1 in control MDCKII cells and 1.9 in MDCKII-BCRP cells. The B-A/A-B ratio for doravirine in BCRP-expressing cells did not decrease in the presence of the BCRP inhibitor Ko143, indicating that doravirine is not a substrate of human BCRP. The B-A/A-B ratio for [^{3}H]prasozin was 4.7 in BCRP-expressing cells and decreased to 1.4 in the presence of Ko143, confirming the functionality of the assay.

(ii) Uptake by OATP1B1 and OATP1B3. In the presence of an inhibitor cocktail designed to fully inhibit OATP1B1, OATP1B3, Na^+-taurocholate cotransporting polypeptide (NTCP), and OCT1, levels of uptake of [^{3}H]doravirine into human hepatocytes were reduced 1.1-, 1.2-, and 1.4-fold after 1, 2, and 5 min, respectively, relative to that of the control (Fig. 3A). In the same studies, the levels of uptake of 1 μM [^{3}H]estradiol 17β-glucuronide ([^{3}H]$E_2$17βG), 5 nM [^{3}H]cholecystokinin 8 ([^{3}H]CCK8), 1 μM [^{3}H]taurocholic acid ([^{3}H]TCA), and 1 μM [^{14}C]tetraethylammonium, known substrates of OATP1B1, OATP1B3, NTCP, and OCT1, respectively, were reduced 4.0- to 12.5-fold in the presence of the cocktail inhibitor relative to the control (see Table S1 in the supplemental material), confirming the functionality of the assay.

The levels of uptake of doravirine into HEK293 cells stably expressing OATP1B1 or OATP1B3 are shown in Fig. 3B and C, respectively. Rapid, time-dependent uptake of doravirine into control cells was observed, likely as a result of passive permeability, with similar uptake into OATP1B1- and OATP1B3-expressing cells. In the same studies, levels of uptake of the OATP1B1 substrate [^{3}H]$E_2$17βG and the OATP1B3 substrate [^{3}H]CCK8 were 51- and 45-fold higher in the OATP1B1- and OATP1B3-transfected cells than in

TABLE 1 Bidirectional transport of doravirine across MDCKII cell monolayers expressing human BCRP[a]

Compound(s)	MDCKII-BCRP P_{app} B-A/A-B	MDCKII P_{app} B-A/A-B	MDCKII P_{app} ($\times$ 10^{-6} cm/s)
[^{3}H]prazosin (5 μM)	4.7	1.0	22.7
[^{3}H]prazosin (5 μM) + Ko143 (2 μM)	1.4	1.2	25.4
[^{3}H]doravirine (0.1 μM)	1.9	1.1	10.9
[^{3}H]doravirine (0.1 μM) + Ko143 (2 μM)	2.3	1.7	10.6
[^{3}H]doravirine (1 μM)	1.7	1.1	10.4
[^{3}H]doravirine (1 μM) + Ko143 (2 μM)	2.1	1.3	11.5

[a]BCRP, breast cancer resistance protein; MDCKII, Madin-Darby canine kidney II; MDCKII-BCRP, MDCKII cells expressing human BCRP; P_{app} B-A/A-B, ratio of basolateral-to-apical apparent permeability (P_{app})/apical-to-basolateral P_{app}.

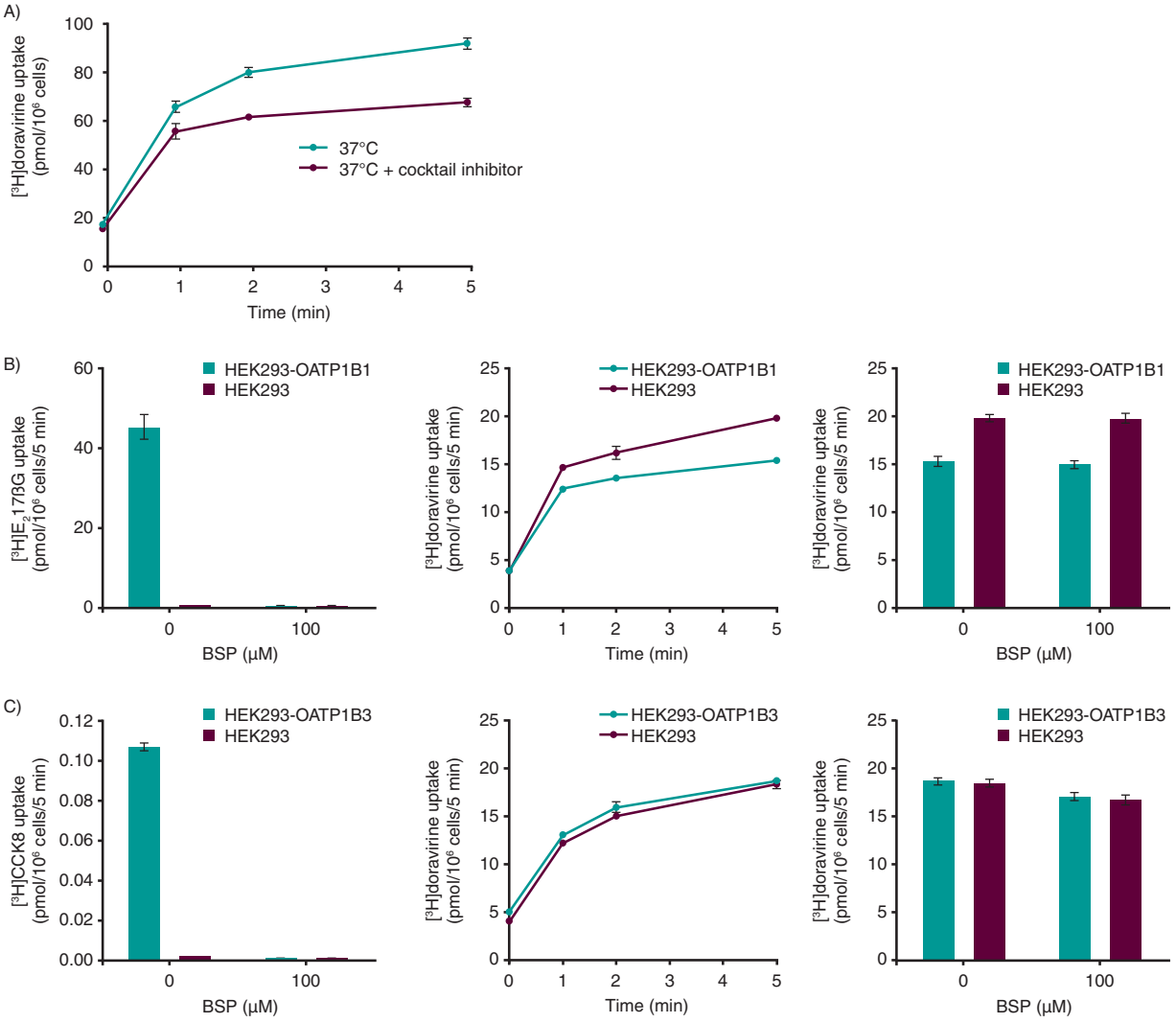

FIG 3 Uptake of doravirine 1 μM into cells. (A) Human hepatocytes in the absence and presence of a cocktail of transporter inhibitors. (B) HEK293 and HEK293-OATP1B1 cells. As a positive control, the inhibitory effect of bromosulfophthalein (BSP; 100 μM) on the uptake of [^{3}H]estradiol 17β-glucuronide ([^{3}H]$E_2$17βG; 1 μM [left]) was also assessed. The middle graph shows the time course of doravirine uptake, and the right graph shows inhibition of doravirine uptake by organic anion transporting polypeptide 1B1 (OATP1B1) inhibitor BSP (100 μM). (C) HEK293 and HEK293-OATP1B3 cells. As a positive control, the inhibitory effect of BSP (100 μM) on the uptake of [^{3}H]cholecystokinin 8 ([^{3}H]CCK8; 5 nM [left]) was also assessed. The middle graph shows the time course of doravirine uptake, and the right graph shows inhibition of doravirine uptake by OATP1B3 inhibitor BSP (100 μM). All data are means ± SEMs.

control cells, respectively, and uptake was effectively inhibited by the OATP inhibitor bromosulfophthalein (BSP).

Inhibition of drug-metabolizing enzymes and transporters by doravirine. (i) Inhibition of CYP isoforms and UGT1A1. The reversible inhibitory effects of doravirine on human liver microsomal activity for CYP1A2, -2B6, -2C8, -2C9, -2C19, -2D6, and -3A4 were evaluated. Doravirine did not inhibit any of the tested CYPs or UGT1A1 (half-maximal inhibitory concentration [IC_{50}] >100 μM) (Table 2). Doravirine did not cause time-dependent inhibition of CYP3A4 activity at 10 and 50 μM (first-order rate constant [k_{obs}] < 0.010 min^{-1} at both concentrations). The k_{obs} for the positive control, mifepristone, was 0.084 min^{-1} at 10 μM, confirming the functionality of the assay.

(ii) Inhibition of drug transporters. Inhibitory effects of doravirine on transporters were determined *in vitro* in stably transfected cells or membrane vesicles containing transporters of interest. The inhibition of drug transporters by doravirine is summarized in Table 3 and a representative example of the full data set shown for OATP1B1 in Fig. 4. Doravirine inhibited BCRP with an IC_{50} value of 51 μM. Doravirine did not inhibit

TABLE 2 Reversible inhibition of CYP enzymes and UGT1A1 in pooled human liver microsomes[a]

CYP	Probe reaction	Incubation time, min	Substrate concn, μM	Control inhibitor (IC_{50}, μM)	IC_{50} of doravirine, μM[b]
1A2	Phenacetin O-deethylation	10	100	α-Naphthoflavone (0.0074)	>100 (0)
2B6	Bupropion hydroxylation	10	180	Ticlopidine (0.74)	>100 (2)
2C8	Amodiaquine N-deethylation	3	4	Montelukast (0.23)	>100 (17)
2C9	Diclofenac 4′-hydroxylation	10	10	Sulfaphenazole (0.74)	>100 (28)
2C19	S-mephenytoin 4′-hydroxylation	20	30	Benzylnirvanol (0.20)	>100 (46)
2D6	Dextromethorphan O-demethylation	20	10	Quinidine (0.083)	>100 (7)
3A4	Midazolam 1′-hydroxylation	3	3	Ketoconazole (0.027)	>100 (0)
3A4	Testosterone 6β-hydroxylation	10	50	Ketoconazole (0.022)	>100 (35)
UGT1A1	Estradiol 3-O-glucuronidation	20	20	Nicardipine (3.2)	>100 (27)

[a]CYP, cytochrome P450; IC_{50}, half-maximal inhibitory concentration; UGT1A1, UDP-glucuronosyltransferase 1A1.
[b]Values in parentheses represent the mean percent inhibition observed at 100 μM.

P-gp-mediated transport of digoxin over the concentration range tested (0.3 to 100 μM). OATP1B1- and OATP1B3-mediated uptake was inhibited by doravirine with IC_{50} values of 39 and 31 μM, respectively. As shown in Fig. 4A, the positive-control inhibitor, cyclosporine A (CsA), effectively inhibited OATP1B1-mediated [^{3}H]pitavastatin uptake, confirming the functionality of the assay. Doravirine did not demonstrate concentration-dependent inhibition of BSEP-mediated TCA uptake. Doravirine inhibited 13% of OAT1-mediated cidofovir uptake at 75 μM, the maximum concentration tested; thus, the estimated IC_{50} value is >75 μM. OAT3 and OCT2 were inhibited by doravirine with IC_{50} values of 16 and 67 μM, respectively. Doravirine inhibited 28% and 39% of MATE1- and MATE2K-mediated metformin uptake, respectively, at 50 μM, the highest concentration tested.

Induction of CYP1A2, CYP2B6, and CYP3A4. Doravirine did not induce CYP1A2 or CYP2B6 mRNA or enzyme activity at concentrations up to 20 μM in human hepatocytes (Table 4). Doravirine induced CYP3A4 mRNA only at concentrations of 10 μM or higher, although the effect was small (3.1% to 20.3% relative to that for the positive control, 10 μM rifampin, at 10 or 20 μM), with no corresponding effect on CYP3A4 enzyme activity.

DISCUSSION

The use of *in vitro* studies to investigate the potential risk of pharmacokinetic interactions has enabled the pharmaceutical industry to make more informed decisions on the clinical development of new drugs. In addition, regulatory agencies recommend the use of *in vitro* studies to evaluate the potential for new pharmaceutical products to perpetrate or be the victim of pharmacokinetic drug interactions when coadministered with other drugs (10, 11). *In vitro* characterization of the drug interaction profile for new

TABLE 3 Effect of doravirine on the activity of human uptake and efflux transporters[a]

Transporter	Substrate (concn, μM)	Maximum concn of doravirine tested (μM)	IC_{50} of doravirine (μM)[b]
BCRP	Methotrexate (10)	75	51 $\pm$ 4
P-gp	Digoxin (0.1)	100	>100 (3)
OATP1B1	Pitavastatin (0.1)	75	39 $\pm$ 2
OATP1B3	Bromosulfophthalein (0.1)	75	31 $\pm$ 4
BSEP	Taurochloric acid (1)	50	>50 (0)
OAT1	Cidofovir (1)	75	>75 (13)
OAT3	Estrone sulfate (1)	75	16.0 $\pm$ 0.7
OCT2	Metformin (10)	75	67 $\pm$ 9
MATE1	Metformin (5)	50	>50 (28)
MATE2K	Metformin (5)	50	>50 (39)

[a]BCRP, breast cancer resistance protein; BSEP, bile salt extrusion pump; IC_{50}, half-maximal inhibitory concentration; MATE, multidrug and toxin extrusion protein; OAT, organic anion transporter; OATP, organic anion transporting polypeptide; OCT, organic cation transporter; P-gp, P-glycoprotein.
[b]IC_{50} values are expressed as mean $\pm$ SEM. Values in parentheses represent the mean percent inhibition at the maximal concentration tested when the IC_{50} was above it.

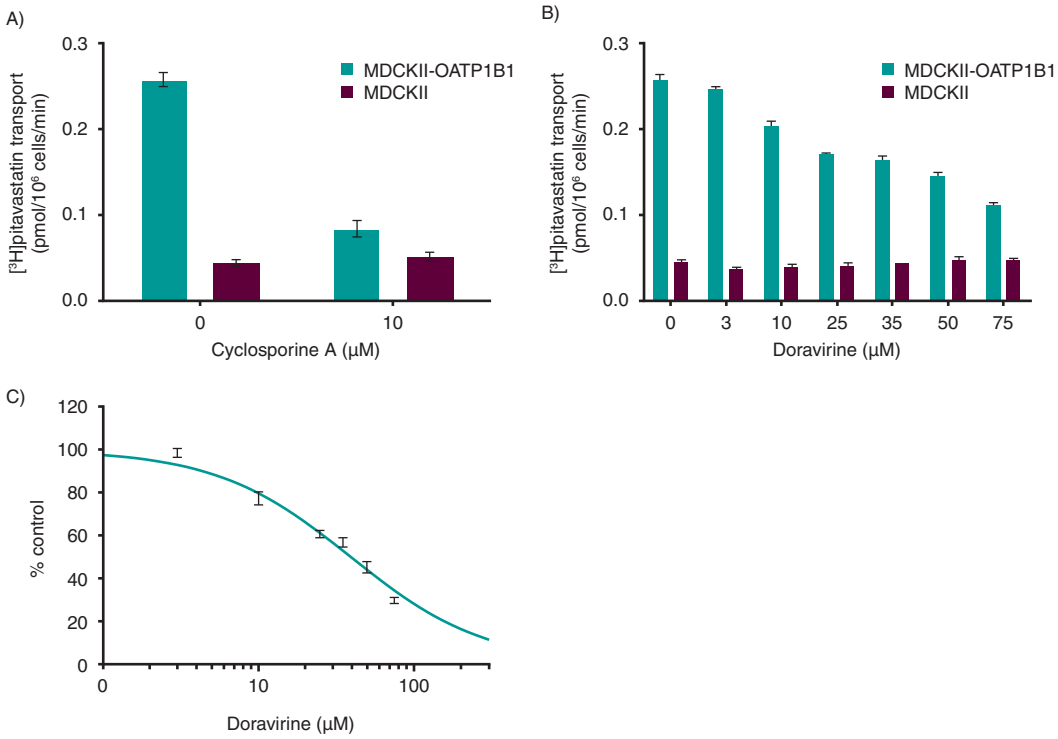

FIG 4 Inhibition of organic anion transporting polypeptide 1B1 (OATP1B1) by doravirine. (A) As a positive control, the inhibitory effect of cyclosporine A (CsA; 10 μM) on the uptake of [^{3}H]pitavastatin (0.1 μM) in OATP1B1 stably transfected MDCKII cells was assessed. (B) Inhibitory effect of doravirine on the uptake of [^{3}H]pitavastatin (0.1 μM) in OATP1B1 stably transfected MDCKII cells. (C) Doravirine inhibition of OATP1B1-mediated [^{3}H]pitavastatin (0.1 μM) uptake (percentage of control). All data are means ± SEMs.

drug entities is used to guide the design and timing of clinical trials and to support product labeling; such data can inform risk assessments regarding the potential for interactions with concomitant medications in the clinical setting.

The results presented here provide a detailed *in vitro* evaluation of the drug interaction profile for doravirine. Further to previous results showing that CYP3A enzymes (specifically, CYP3A4 and CYP3A5) catalyze the oxidative metabolism of doravirine (7), kinetic studies indicated an approximate 20-fold-higher catalytic efficiency for CYP3A4 than for CYP3A5. Clinical trials have demonstrated that doravirine is subject to drug interactions with CYP3A inhibitors and inducers (12–15). Multiple dosing of the CYP3A inhibitors ketoconazole and ritonavir increased exposure (area under the concentration-time curve from time zero to infinity [AUC_{0-inf}]) to doravirine 3.1- and 3.5-fold, respectively, relative to the doravirine AUC value following the administration of doravirine alone (12, 13). In addition, multiple-dose administration of the CYP3A4 inducers rifabutin and rifampin reduced AUC_{0-inf} by 50% and 88%, respectively (14, 15). The higher efficiency of CYP3A4

TABLE 4 Induction of CYP1A2, -2B6, and -3A4 by doravirine and known CYP inducers in cultured human hepatocytes[a]

			Fold change					
			Donor 1		Donor 2		Donor 3	
Treatment	Concn (μM)	Enzyme	mRNA	Enzyme activity	mRNA	Enzyme activity	mRNA	Enzyme activity
Omeprazole	50	1A2	31.3	22	32.1	8.9	21.3	13
Doravirine	20	1A2	1.2	1	1.9	1.8	1	1.1
Phenobarbital	1,000	2B6	15.7	7.3	18.5	7.2	14.0	13.7
Doravirine	20	2B6	1.9	1	1.5	1.1	1.2	0.8
Rifampin	10	3A4	8.8	5.9	16.8	9	18.2	19.7
Doravirine	20	3A4	1.4	1	4.2	1	3.8	0.9

[a]CYP, cytochrome P450.

in catalyzing the metabolism of doravirine, the *in vivo* metabolism data revealing that oxidative metabolism is the major route of elimination of doravirine (7), and the predominant expression of CYP3A4 in intestine and liver (16) suggests that CYP3A4 is the major enzyme responsible for the elimination of doravirine in humans, while CYP3A5 metabolizes doravirine with a lower efficiency.

Transporter-mediated drug interactions have also received significant attention in recent years, and regulatory agencies require the investigation of the importance of active uptake and secretion in the disposition of new chemical entities, as well as the study of the potential to inhibit major drug transporters *in vitro* (10, 11). Previous results from clinical evaluation of the absorption, distribution, and elimination of doravirine indicated that active transport mechanisms are unlikely to play a significant role in the disposition of doravirine (7). In line with those findings, doravirine was not found to be a substrate of several major drug transporters. Doravirine was not a substrate of human BCRP *in vitro*, and studies with cryopreserved human hepatocytes showed reduced uptake of doravirine by a maximum of only 1.4-fold in the presence of a cocktail of transport inhibitors designed to fully inhibit OATP1B1, OATP1B3, NTCP, and OCT1. Passive permeability appeared to be the major driver of uptake of doravirine into hepatocytes. Doravirine was also evaluated as a substrate of OATP1B1 and OATP1B3 in stably transfected HEK293 cells. Rapid, time-dependent uptake of doravirine into control cells was observed, likely as a result of passive permeability. Uptake in transfected cells was similar to that in control cells, indicating that doravirine was likely not a substrate of OATP1B1 and OATP1B3. Further evidence has been provided by the clinical drug-drug interaction trial of doravirine with rifampin (14), a drug which after multiple-dose administration induces CYP3A and intestinal P-gp, and after single-dose administration inhibits intestinal P-gp and OATP-mediated uptake of drugs in the liver (14, 17–19). After single-dose administration of rifampin, doravirine AUC_{0-inf} and plasma concentration at 24 h postdose (C_{24}) were comparable in the absence and presence of rifampin, indicating that inhibition of OATP uptake transporters has little impact on doravirine pharmacokinetics (14). Doravirine was not evaluated as a substrate of major renal transporters, as renal excretion is not a significant route of elimination in humans (20).

In order to further characterize the drug interaction profile of doravirine, its ability to modulate major metabolic enzymes and transporters was evaluated *in vitro*. Doravirine was not a reversible inhibitor of CYP1A2, CYP2B6, CYP2C8, CYP2C9, CYP2C19, CYP2D6, CYP3A4, or UGT1A1 (IC_{50} values were all >100 μM), nor was it a time-dependent inhibitor of CYP3A4.

The induction potential of doravirine was evaluated in human hepatocytes from 3 donors, in which it did not increase CYP1A2 or CYP2B6 mRNA or enzyme activity, at concentrations above the clinical maximum plasma concentration (C_{max}) (2.3 μM) (4). An increase in CYP3A4 mRNA was observed at 10 and 20 μM, but the effect was small relative to that of the positive control and did not have a corresponding effect on enzyme activity. In agreement, clinical evaluation of the effect of multiple once-daily doses of doravirine at 120 mg showed that there was no significant effect on the exposure of the sensitive CYP3A substrate midazolam in healthy subjects (20).

Evaluation of doravirine as an inhibitor of major drug transporters indicated a low potential for interactions with substrates of BCRP, P-gp, OATP1B1, OATP1B3, BSEP, OAT1, OAT3, OCT2, MATE1, and MATE2K. Doravirine was an inhibitor of BCRP, with an *in vitro* IC_{50} of 51 μM, more than 50-fold above the unbound C_{max}, and thus, systemic interactions with BCRP are unlikely. However, doravirine could inhibit the intestinal efflux of substrates of this transporter and increase their exposure. The theoretical gut lumen concentrations of doravirine (400 μg/ml or 940 μM, assuming complete dissolution of the 100-mg dose in 250 ml of intestinal fluid), at the therapeutic dose, exceed the *in vitro* IC_{50} value. However, the solubility of doravirine is limited. *In vitro*, the solubility of doravirine is 120 μg/ml (282 μM [data on file]) and not dependent on pH, so actual concentrations in the gut lumen are unlikely to exceed this. However, the clinical relevance of such an interaction is anticipated to be low. In a clinical trial, coadministration of the BCRP substrate dolute-

gravir with doravirine at 200 mg increased the steady-state plasma levels of dolutegravir (AUC from time zero to 24 h, C_{max}, and C_{24}) by approximately 30%; this effect was not considered clinically meaningful (21).

Doravirine did not inhibit P-gp at concentrations up to 100 μM and is not anticipated to alter the pharmacokinetics of P-gp substrates via systemic interactions. Inhibition of intestinal P-gp is unlikely if, as indicated above, gut lumen concentrations of doravirine approach the estimated aqueous solubility of 282 μM. Attempts to test doravirine inhibition of P-gp at 300 μM failed due to precipitation of doravirine in the assay media. Thus, although inhibition of gut P-gp cannot be excluded, it is likely to be limited by the solubility of doravirine and be of no clinical relevance.

As OATP1B1 and OATP1B3 are located at the sinusoidal membrane of hepatocytes (22), the *in vitro* inhibition of OATP1B1 and OATP1B3 needs to be put in the context of the maximum unbound drug concentration at the inlet of the liver during the absorption phase (23). The hepatic inlet unbound C_{max} after an oral 100-mg dose of doravirine was estimated to be $\sim$3 μM, assuming that the fraction absorbed was approximately 0.67 (based on the bioavailability of the 100-mg tablet [4]) and that the rate of absorption was 0.14 h^{-1} and the C_{max} was 2.3 μM, with a hepatic blood flow of 90 liters/h (based on the population pharmacokinetic analysis [38]) and unbound fraction of 0.24 (7). In this context, the IC_{50} values of 39 and 31 μM in the OATP1B1 and OATP1B3 *in vitro* assays, respectively, are approximately 13- and 10-fold above the hepatic inlet unbound C_{max}, and the risk for doravirine to cause drug interactions via inhibition of these transporters is low. In a clinical trial, doravirine did not have a clinically meaningful effect on the pharmacokinetics of atorvastatin, an OATP1B1 substrate (24).

The disposition of bile salts involves the concerted activity of various transporters, including BSEP, which resides in the apical membrane of the hepatocyte (25, 26). Association of BSEP inhibition with drug-related liver injury is still a matter of discussion (27, 28). Doravirine did not inhibit BSEP-mediated transport at concentrations up to 50 μM *in vitro* and is therefore unlikely to affect the disposition of substrates of this transporter. Doravirine is also unlikely to interfere with the active uptake and secretion of drugs in the kidney. Given the IC_{50} values of $>$75, 16, and 67 μM for OAT1, OAT3, and OCT2, respectively, and that the unbound C_{max} at therapeutic concentrations is likely below 1 μM (based on clinical C_{max} and unbound fraction of 0.24 [7]), the *in vitro* IC_{50} values for these transporters are approximately 20-fold the doravirine plasma concentration or higher. Therefore, systemic drug interactions via these transporters are also unlikely. IC_{50} values for inhibition of MATE1 and MATE2K by doravirine were $>$50 μM, indicating that the risk for interaction of doravirine with substrates of these transporters is also low. In a clinical trial, the pharmacokinetics of tenofovir, an OAT1/3 substrate (29), administered as TDF with lamivudine, were similar when administered with and without doravirine (M. S. Anderson, J. Gilmartin, L. Fan, K. L. Yee, W. K. Kraft, I. Triantafyllou, C. Reitmann, Y. Guo, R. Liu, M. Iwamoto, and M. O. Behm, submitted for publication). Likewise, the pharmacokinetics of lamivudine, a substrate of MATE1, MATE2K, and OCT2 (30), administered with TDF were similar when administered with and without doravirine (Anderson et al., submitted). Furthermore, doravirine also did not have a clinically relevant effect on the pharmacokinetics of metformin, a substrate of OCT2, MATE1, and MATE2K (R. I. Sanchez, K. L. Yee, L. Fan, D. Cislak, M. Martell, H. R. Jordan, M. Iwamoto, and S. Khalilieh, submitted for publication).

In summary, these *in vitro* findings indicate that the major elimination pathway of doravirine is CYP3A4-mediated metabolism, while CYP3A5 involvement is minor. In agreement with these results, clinical trials demonstrate that doravirine is subject to drug interactions with CYP3A inhibitors and inducers but is unlikely to be affected by inhibitors of other enzymes or of major drug transporters (7). Doravirine was not a substrate of BCRP and likely not a substrate of OATP1B1 or -1B3. The *in vitro* findings also indicate that doravirine is unlikely to be the perpetrator of drug interactions via major drug-metabolizing enzymes and transporters; subsequent clinical trials have confirmed that doravirine has minimal drug-drug interactions.

MATERIALS AND METHODS

Kinetic characterization of CYP3A4- and CYP3A5-catalyzed oxidation of doravirine. (i) Determination of fraction unbound for kinetics studies. The unbound fraction of doravirine (Merck & Co., Inc., West Point, PA) in rCYP3A4 and rCYP3A5 incubation mixtures was determined via ultracentrifugation. Triplicate samples of either rCYP3A4 (25 pmol/ml) or rCYP3A5 (100 pmol/ml) (Corning Incorporated Life Sciences, Tewksbury, MA) were prepared in 100 mM potassium phosphate buffer (pH 7.4) containing 1 mM $MgCl_2$ with final doravirine concentrations of 0.5 and 5 μM. The samples were incubated at 37°C for 30 min, and aliquots (1.1 ml) were transferred into polyallomer Microfuge tubes (Beckman Instruments, Palo Alto, CA). Control samples were prepared by removing a 0.1-ml aliquot from each sample and adding 0.1 ml of acetonitrile, containing an internal standard mixture. The remaining samples were centrifuged at 182,000 $\times$ *g* for 1 h using a Beckman Optima Max ultracentrifuge (Beckman Instruments). Aliquots of the resulting supernatants were removed and mixed with an equal volume of acetonitrile. Following centrifugation at 3,500 $\times$ *g* for 10 min, aliquots of the supernatants were subjected to liquid chromatography-tandem mass spectrometry (LC-MS/MS) analysis using a Waters Acquity (Milford, MA) ultraperformance liquid chromatography (UPLC) system interfaced to an API-4500 mass spectrometer utilizing the turbo ionspray interface (AB Sciex, Framingham, MA) in the positive-ion mode. Chromatographic separation was achieved with a gradient elution on a Waters Xselect HSS T3 UPLC column (2.1-mm inside diameter [ID] by 50-mm length; 2.5-μm particle size) with mobile phases consisting of 0.1% formic acid in water (solvent A) and 0.1% formic acid in acetonitrile (solvent B). The fraction unbound was calculated as the concentration in the supernatant divided by the concentration in the control.

(ii) CYP3A4 and CYP3A5 kinetics studies. Doravirine (0.3 to 50 μM) was preincubated, in triplicate, for 10 min at 37°C with either rCYP3A4 or rCYP3A5 as described above. The reactions were initiated by addition of NADPH (1 mM) and allowed to proceed for 15 min where the formation rate of M9 was linear with respect to rCYP concentration and incubation time. Reactions were terminated by addition of an equal volume of acetonitrile containing an internal standard mixture, followed by centrifugation at 3,500 $\times$ *g* for 10 min. The supernatants were subjected to LC-MS/MS analysis to determine the concentration of M9, using a Thermo Transcend LX2 multiplexed UPLC system, with Agilent 1260 Infinity pumps and an HTS PAL CTC autosampler, interfaced to an API-6500+ QTrap mass spectrometer using the turbo ionspray interface (AB Sciex, Framingham, MA) in positive-ion mode. Chromatographic separation of M9 was achieved on a Waters XSelect HSS XP T3 UPLC column as described above.

Enzyme kinetics data were analyzed to estimate the K_m and V_{max} values of M9 formation. The velocity versus substrate concentration data were fit to the Michaelis-Menten equation to obtain approximate values for $K_{m,app}$ and V_{max} for both rCYP3A4 and rCYP3A5 as described by Sjögren et al. (31). The K_m values were subsequently determined by correcting the $K_{m,app}$ for binding in the incubation (31), and the CL_{int} values were then calculated from K_m and V_{max} (32).

Drug transporters involved in the disposition of doravirine. (i) Efflux of doravirine by BCRP. Bidirectional transport of [^{3}H]doravirine (Labeled Compound Synthesis Department, Merck & Co., Inc., Rahway, NJ) was measured across MDCKII and MDCKII-BCRP cells using a previously described method (33), with the exception that cells were cultured in 96-well Transwell culture plates (Millipore Corp., Billerica, MA). The experiments were performed in triplicate. The P_{app} values and B-A/A-B efflux ratios were calculated as previously described (34).

(ii) Uptake by OATP1B1 and OATP1B3. Uptake of [^{3}H]doravirine into cryopreserved human hepatocytes (20-donor pool; Bioreclamation IVT, Baltimore, MD) was evaluated in the absence and presence of a transporter inhibitor cocktail (CsA [10 μM] plus rifamycin SV [10 μM] plus rifampin [100 μM] plus quinidine [50 μM]) at 37°C as described previously (33, 35).

The uptake of [^{3}H]doravirine into HEK293 cells transiently transfected with OATP1B1 and OATP1B3 (Corning Life Sciences, Corning, NY) was measured. Briefly, 24 h prior to the experiment, control or transfected cells were treated with sodium butyrate (5 mM) to increase the OATP expression. Cells were dislodged with trypsin EDTA and resuspended in Hanks' balanced salt solution (HBSS) with HEPES (10 mM; pH 7.4). Cells were then suspended in 96-well glass-coated plates (Arctic White LLC, Bethlehem, PA) at a density of 0.2 $\times$ 10^6/well in 125 μl of HBSS. Uptake was initiated by addition of 125 μl of [^{3}H]doravirine or a positive-control substrate, [^{3}H]$E_2$17βG for OATP1B1 or [^{3}H]CCK8 for OATP1B3, with and without BSP, a known OATP1B inhibitor, at final concentrations of 1 μM [^{3}H]doravirine, 1 μM [^{3}H]$E_2$17βG, 5 nM [^{3}H]CCK8, and 100 μM BSP. Cells were incubated for the desired time at 37°C, and the uptake was stopped by the addition of ice-cold phosphate-buffered saline (PBS). Cells were washed three times in PBS and radioactivity was determined as previously described (36). The experiment was performed in triplicate.

Inhibition of drug-metabolizing enzymes and transporters by doravirine. (i) Inhibition of CYP isozymes. A reversible CYP inhibition study was conducted at Advion Biosciences Inc. (Ithaca, NY). Pooled human liver microsomes (0.25 mg/ml; BD Biosciences, San Jose, CA) were incubated at 37°C in a reaction mixture (0.2-ml final volume) containing the appropriate CYP probe substrate and doravirine (0.05 to 100 μM) in potassium phosphate buffer (100 mM; pH 7.4) with 3.14 mM $MgCl_2$ and an NADPH-generating system (glucose-6-phosphate [2.82 mM], NADP [1.25 mM], and glucose-6-phosphate dehydrogenase [1.34 U/ml]). The substrate concentrations ranged from 3 to 180 μM (near their K_m values), and incubation times were between 3 and 20 min (Table 2). The reactions were terminated by adding 200 μl of methanol for the CYP2D6 and CYP3A4 assays and 50 μl of 50% acetonitrile–2.5% formic acid–0.1% methanol (vol/vol/vol in water) for all other assays. Stop solutions contained the appropriate internal standard. CYP2C8 samples were diluted 1:3 with 10% acetonitrile–0.5% formic acid (vol/vol in water). The samples were centrifuged for 10 min at 2,500 $\times$ *g* before being transferred to a clean 96-well plate and

analyzed by LC-MS/MS using an API-3000 mass spectrometer utilizing the turbo ionspray interface (AB Sciex, Framingham, MA) in the positive-ion mode. The experiment was performed in triplicate.

Chromatographic separation was achieved with gradient elution using a Luna C18(2) high-performance liquid chromatography column (2-mm ID by 50 mm; 5-μm particle size; Phenomenex, Torrance, CA) with mobile phases consisting of 0.05% formic acid in water (solvent A) and 0.05% formic acid in 95:5 acetonitrile-water (vol/vol; solvent B).

IC_{50} values were calculated using SigmaPlot v11.0 (Systat Software Inc., San Jose, CA) by nonlinear regression.

(ii) Time-dependent inhibition of CYP3A4. Pooled ($n = 150$) human liver microsomes (1 mg/ml; BD Biosciences, San Jose, CA) were preincubated for 5 to 45 min at 37°C with doravirine (10 and 50 μM) in potassium phosphate buffer (100 mM; pH 7.4) containing EDTA (1 mM), $MgCl_2$ (6 mM), and an NADPH-generating system (single incubation at each time point). The incubation mixtures were diluted 10-fold with the same buffer containing testosterone (250 μM) and incubated for a further 10 min to monitor the 6β-hydroxylation of testosterone. The reaction was stopped, samples were centrifuged for 10 min at 3,200 $\times$ *g*, 100 μl of the supernatant was diluted with 50 μl of 0.05% formic acid, and samples were analyzed by LC-MS/MS using an API-4000 mass spectrometer utilizing the turbo ionspray interface (AB Sciex, Framingham, MA) in the positive-ion mode. Chromatographic separation of 6β-hydroxytestosterone was achieved as described above.

k_{obs} values for inactivation were calculated from the negative slope of the lines by linear regression analysis of the natural logarithm of the remaining activity as a function of time.

(iii) Inhibition of UGT1A1. Pooled human liver microsomes (0.5 mg/ml) were incubated with estradiol (20 μM), a substrate for UGT1A1, UDP glucuronic acid (5 mM), $MgCl_2$ (9 mM), and alamethicin (25 μg/ml) in 200 μl of HEPES buffer (81 mM; pH 7.0) at 37°C for 20 min. Estradiol glucuronidation was quantified in the absence and presence of increasing concentrations of doravirine (0.78 to 100 μM) or nicardipine (0.078 to 10 μM), a known inhibitor of UGT1A1. Human liver microsomal protein was precipitated by adding ice-cold methanol (0.2 ml) containing labetalol as the internal standard. Samples were centrifuged at 4,000 $\times$ *g* for 30 min at 4°C, 200 μl of the supernatant was diluted with 100 μl of 0.05% formic acid, and samples analyzed by LC-MS/MS using an API-4000 triple mass spectrometer utilizing the turbo ionspray interface in the negative-ion mode. Chromatographic separation of estradiol-3-glucuronide was achieved using gradient elution using a Symmetry C18 column (4.6 by 100 mm; 3.5-μm particle size; Waters Corp., Milford, MA) with mobile phases consisting of 0.1% formic acid in water (solvent A) and 0.1% formic acid in acetonitrile. The experiment was performed in triplicate.

IC_{50} values were calculated by nonlinear regression analysis using KaleidaGraph (Synergy Software, Reading, PA).

(iv) Inhibition of drug transporters. Inhibition of OATP1B1-, OATP1B3-, OAT1-, and OAT3-mediated uptake of probe substrates (as described in Table 3) was determined in MDCKII cells stably expressing the transporter of interest (MDCKII-OATP1B1, MDCKII-OATP1B3, MDCKII-OAT1, or MDCKII-OAT3) as described previously (33–36), in the presence and absence of doravirine or a positive-control inhibitor. Similarly, inhibition of OCT2-, MATE1-, and MATE2K-mediated uptake was determined in CHO-K1-OCT2, CHO-K1-MATE1, and MDCKII-MATE2K cells as described previously (36). The experiments were performed in triplicate.

The inhibitory effect of doravirine on ATP-dependent [^{3}H]methotrexate (10 μM) uptake was tested in membrane vesicles containing human BCRP as described previously (36), with preincubation in the presence and absence of doravirine or Ko143 (5 μM), a known BCRP inhibitor, for 5 min at 37°C. The inhibition of BSEP was studied using the same methodology, using [^{3}H]TCA (1 μM) as the probe substrate and atorvastatin (100 μM) as the positive-control inhibitor. The experiments were performed in triplicate.

Inhibition of P-gp was assessed at Corning Life Sciences, Woburn, MA, in LLC-MDR1 cells cultured in 24-well multiwell insert plates at 37°C. Doravirine (0.3 to 300 μM) was tested as an inhibitor of [^{3}H]digoxin (0.1 μM) transport, with cyclosporine (10 μM) as a positive control for P-gp inhibition. Receiver solution was prepared by adding aliquots of inhibitor stock solution to transport buffer, HBSS with 10 mM HEPES (pH 7.4), with a final organic solvent concentration of $\leq$1%. Dosing solutions were prepared by diluting aliquots of [^{3}H]digoxin and doravirine in transport buffer, and 500 μl was added to either the apical (A) or basolateral (B) compartment, with matching receiver solution added to the opposite compartment. At 90 min, samples were taken from both sides and scintillant (UltimaFlo-M, PerkinElmer, Boston, MA) was added. Radioactivity was determined by liquid scintillation counting in a Beckman LS6500 scintillation counter (Beckman, Fullerton, CA). The experiments were performed in triplicate.

IC_{50} values for inhibition of transporter-mediated uptake were calculated by nonlinear regression as described previously (36).

Induction of CYP1A2, CYP2B6, and CYP3A4. Cryopreserved human hepatocytes prepared from three single donors (Corning Life Sciences, Woburn, MA) were used to investigate the induction potential of doravirine. As detailed previously (37), the hepatocytes were thawed, plated, and cultured for 24 h in plating medium prior to initiation of the study. The hepatocytes were treated for 48 h with a vehicle control, doravirine (0.1 to 20 μM), or the positive-control inducer (omeprazole [50 μM] for CYP1A2, phenobarbital [1,000 μM] for CYP2B6, or rifampin [10 μM] for CYP3A4). At the end of the 48-h incubation, whole-cell-based enzyme activity was evaluated by monitoring the rate of phenacetin O-demethylation (CYP1A2), bupropion hydroxylation (CYP2B6), or testosterone 6β-hydroxylation (CYP3A4) using LC-MS/MS analysis. Total RNA was isolated for quantitative PCR analysis of mRNA expression as described previously (37). The experiments were performed in triplicate.

LC-MS/MS analysis was performed using a Thermo Transcend LX2 Multiplexed UPLC system with an HTS PAL CTC autosampler (Leap Technologies, Carrboro, NC) interfaced to an API-4000 mass spectrom-

eter using the turbo ionspray interface in positive-ion mode. Chromatographic separation was achieved on a Waters C8 column (2.1 mm by 30 mm; 1.7-μm particle size; Waters Corp., Milford, MA) using a step gradient and mobile phases consisting of 0.1% formic acid in water (solvent A) and 0.1% formic acid in acetonitrile (solvent B).

Data availability. Available data can be obtained by contacting the corresponding author. Any data that are reasonably requested will be made available in a timely fashion to members of the scientific community with as few restrictions as feasible for noncommercial purposes. Subject to requirements or limitations imposed by local and/or U.S. government laws and regulations, we will make every effort to provide to those that request it additional information on the sources of materials used in the studies described here.

SUPPLEMENTAL MATERIAL

Supplemental material for this article may be found at https://doi.org/10.1128/AAC.02492-18.

SUPPLEMENTAL FILE 1, PDF file, 0.2 MB.

ACKNOWLEDGMENTS

Funding for this research was provided by Merck Sharp & Dohme Corp., a subsidiary of Merck & Co., Inc., Kenilworth, NJ.

K.B., K.L.F., R.H., B.L., J.P., D.J.N., M.L., G.H.C., and R.I.S. are current or former employees of Merck Sharp & Dohme Corp., a subsidiary of Merck & Co., Inc., Kenilworth, NJ, and may own stock and/or stock options in Merck & Co., Inc., Kenilworth, NJ.

K.B., R.H., B.L., M.L., and R.I.S. substantially contributed to the conception, design or planning of the study. K.L.F., R.H., J.P., D.J.N., M.L., and G.H.C. substantially contributed to the acquisition of the data. K.L.F., R.H., B.L., J.P., M.L., G.H.C., and R.I.S. subtantially contributed to analysis of the data. K.B., K.L.F., R.H., J.P., M.L., G.H.C., and R.I.S. substantially contributed to interpretation of the results. All authors critically reviewed or revised the manuscript for important intellectual content, and K.B., R.H., and R.I.S. substantially contributed to drafting of the manuscript. All authors reviewed and approved the version of the manuscript to be submitted.

We thank Xiaoyan Chu for assistance with the OATP1B1/1B3 and hepatocyte uptake studies and the MATE1, MATE2K, and BSEP inhibition studies.

Medical writing assistance, under the direction of the authors, was provided by Annette Smith of CMC AFFINITY, a division of McCann Health Medical Communications Ltd., Macclesfield, UK, in accordance with good publication practice (GPP3) guidelines. This assistance was funded by Merck Sharp & Dohme Corp., a subsidiary of Merck & Co., Inc., Kenilworth, NJ. We thank Donald Tweedie (Merck & Co., Inc.) for critical review of the manuscript.

REFERENCES

1. Marcus JL, Chao CR, Leyden WA, Xu L, Quesenberry CP, Jr, Klein DB, Towner WJ, Horberg MA, Silverberg MJ. 2016. Narrowing the gap in life expectancy between HIV-infected and HIV-uninfected individuals with access to care. J Acquir Immune Defic Syndr 73:39–46. https://doi.org/10.1097/QAI.0000000000001014.
2. Guaraldi G, Orlando G, Zona S, Menozzi M, Carli F, Garlassi E, Berti A, Rossi E, Roverato A, Palella F. 2011. Premature age-related comorbidities among HIV-infected persons compared with the general population. Clin Infect Dis 53:1120–1126. https://doi.org/10.1093/cid/cir627.
3. Friedman EE, Duffus WA. 2016. Chronic health conditions in Medicare beneficiaries 65 years old, and older with HIV infection. AIDS 30:2529–2536. https://doi.org/10.1097/QAD.0000000000001215.
4. Merck & Co., Inc. 2018. PIFELTRO (doravirine) prescribing information. https://www.merck.com/product/usa/pi_circulars/p/pifeltro/pifeltro_pi.pdf.
5. Merck & Co., Inc. 2018. DELSTRIGO (doravirine, lamivudine, and tenofovir disoproxil fumarate) prescribing information. https://www.merck.com/product/usa/pi_circulars/d/delstrigo/delstrigo_pi.pdf.
6. Feng M, Sachs NA, Xu M, Grobler J, Blair W, Hazuda DJ, Miller MD, Lai M-T. 2016. Doravirine suppresses common nonnucleoside reverse transcriptase inhibitor-associated mutants at clinically relevant concentrations. Antimicrob Agents Chemother 60:2241–2247. https://doi.org/10.1128/AAC.02650-15.
7. Sanchez RI, Fillgrove KL, Yee KL, Liang Y, Lu B, Tatavarti A, Liu R, Anderson MS, Behm MO, Fan L, Li Y, Butterton JR, Iwamoto M, Khalilieh SG. 2018. Characterisation of the absorption, distribution, metabolism, excretion and mass balance of doravirine, a non-nucleoside reverse transcriptase inhibitor in humans. Xenobiotica https://doi.org/10.1080/00498254.2018.1451667.
8. Orkin C, Squires KE, Molina JM, Sax PE, Wong WW, Sussmann O, Kaplan R, Lupinacci L, Rodgers A, Xu X, Lin G, Kumar S, Sklar P, Nguyen BY, Hanna GJ, Hwang C, Martin EA, DRIVE-AHEAD Study Group. 2019. Doravirine/lamivudine/tenofovir disoproxil fumarate is non-inferior to efavirenz/emtricitabine/tenofovir disoproxil fumarate in treatment-naive adults with human immunodeficiency virus-1 infection: week 48 results of the DRIVE-AHEAD Trial. Clin Infect Dis 68:535–544. https://doi.org/10.1093/cid/ciy540.
9. Molina JM, Squires K, Sax PE, Cahn P, Lombaard J, DeJesus E, Lai MT, Xu X, Rodgers A, Lupinacci L, Kumar S, Sklar P, Nguyen BY, Hanna GJ, Hwang C, DRIVE-FORWARD Study Group. 2018. Doravirine versus ritonavir-boosted darunavir in antiretroviral-naive adults with HIV-1 (DRIVE-FORWARD): 48-week results of a randomised, double-blind, phase 3, non-inferiority trial. Lancet HIV 5:e211–e220. https://doi.org/10.1016/S2352-3018(18)30021-3.
10. European Medicines Agency. 2013. Guideline on the investigation of drug interactions. http://www.ema.europa.eu/docs/en_GB/document_library/Scientific_guideline/2012/07/WC500129606.pdf.

11. US Department of Health and Human Services/FDA/Center for Drug Evaluation and Research. 2017. In vitro metabolism- and transporter-mediated drug-drug interaction studies. Guidance for industry. https://www.fda.gov/downloads/Drugs/GuidanceComplianceRegulatoryInformation/Guidances/UCM581965.pdf.
12. Anderson MS, Chung C, Tetteh E, Yee KL, Ying G, Rasmussen S, Wagner JA, Butterton JR. 2015. Effect of ketoconazole on the pharmacokinetics of doravirine (MK-1439), a novel non-nucleoside reverse transcriptase inhibitor for the treatment of HIV-1 infection. Rev Antivir Ther Infect Dis, 16th Int Workshop Clin Pharmacol HIV Hepatitis Ther, Washington, DC.
13. Khalilieh S, Anderson M, Laethem T, Yee K, Sanchez R, Fan L, Sura M, van Bortel L, Van Lancker G, Iwamoto M. 2017. Multiple-dose treatment with ritonavir increases the exposure of doravirine, abstr 412. Conference on Retroviruses and Opportunistic Infections (CROI), 13 to 16 February 2017, Seattle, WA.
14. Yee KL, Khalilieh SG, Sanchez RI, Liu R, Anderson MS, Manthos H, Judge T, Brejda J, Butterton JR. 2017. The effect of single and multiple doses of rifampin on the pharmacokinetics of doravirine in healthy subjects. Clin Drug Investig 37:659–667. https://doi.org/10.1007/s40261-017-0513-4.
15. Khalilieh SG, Yee KL, Sanchez RI, Liu R, Fan L, Martell M, Jordan H, Iwamoto M. 2018. Multiple doses of rifabutin reduce exposure of doravirine in healthy subjects. J Clin Pharmacol 58:1044–1052. https://doi.org/10.1002/jcph.1103.
16. Human Protein Atlas. 2018. CYP3A4. https://www.proteinatlas.org/ENSG00000160868-CYP3A4/tissue.
17. Niemi M, Backman JT, Fromm MF, Neuvonen PJ, Kivistö KT. 2003. Pharmacokinetic interactions with rifampicin: clinical relevance. Clin Pharmacokinet 42:819–850. https://doi.org/10.2165/00003088-200342090-00003.
18. Reitman ML, Chu X, Cai X, Yabut J, Venkatasubramanian R, Zajic S, Stone JA, Ding Y, Witter R, Gibson C, Roupe K, Evers R, Wagner JA, Stoch A. 2011. Rifampin's acute inhibitory and chronic inductive drug interactions: experimental and model-based approaches to drug-drug interaction trial design. Clin Pharmacol Ther 89:234–242. https://doi.org/10.1038/clpt.2010.271.
19. Vavricka SR, Van Montfoort J, Ha HR, Meier PJ, Fattinger K. 2002. Interactions of rifamycin SV and rifampicin with organic anion uptake systems of human liver. Hepatology 36:164–172. https://doi.org/10.1053/jhep.2002.34133.
20. Anderson MS, Gilmartin J, Cilissen C, De Lepeleire I, van Bortel L, Dockendorf MF, Tetteh E, Ancona JK, Liu R, Guo Y, Wagner JA, Butterton JR. 2015. Safety, tolerability and pharmacokinetics of doravirine, a novel HIV non-nucleoside reverse transcriptase inhibitor, after single and multiple doses in healthy subjects. Antivir Ther 20:397–405. https://doi.org/10.3851/IMP2920.
21. Anderson MS, Khalilieh S, Yee KL, Liu R, Fan L, Rizk ML, Shah V, Hussaini A, Song I, Ross LL, Butterton JR. 2017. A two-way steady-state pharmacokinetic interaction study of doravirine (MK-1439) and dolutegravir. Clin Pharmacokinet 56:661–669. https://doi.org/10.1007/s40262-016-0458-4.
22. Konig J, Cui Y, Nies AT, Keppler D. 2000. A novel human organic anion transporting polypeptide localized to the basolateral hepatocyte membrane. Am J Physiol Gastrointest Liver Physiol 278:G156–G164. https://doi.org/10.1152/ajpgi.2000.278.1.G156.
23. Vaidyanathan J, Yoshida K, Arya V, Zhang L. 2016. Comparing various in vitro prediction criteria to assess the potential of a new molecular entity to inhibit organic anion transporting polypeptide 1B1. J Clin Pharmacol 56:S59–S72. https://doi.org/10.1002/jcph.723.
24. Khalilieh S, Yee KL, Sanchez RI, Triantafyllou I, Fan L, Maklad N, Jordan H, Martell M, Iwamoto M. 2017. Results of a doravirine-atorvastatin drug-drug interaction study. Antimicrob Agents Chemother 61:e01364-16. https://doi.org/10.1128/AAC.01364-16.
25. Telbisz Á, Homolya L. 2016. Recent advances in the exploration of the bile salt export pump (BSEP/ABCB11) function. Expert Opin Ther Targets 20:501–514. https://doi.org/10.1517/14728222.2016.1102889.
26. Dawson PA, Lan T, Rao A. 2009. Bile acid transporters. J Lipid Res 50:2340–2357. https://doi.org/10.1194/jlr.R900012-JLR200.
27. Chan R, Benet LZ. 2018. Measures of BSEP inhibition in vitro are not useful predictors of DILI. Toxicol Sci 162:499–508. https://doi.org/10.1093/toxsci/kfx284.
28. Kenna JG, Taskar KS, Battista C, Bourdet DL, Brouwer KLR, Brouwer KR, Dai D, Funk C, Hafey MJ, Lai Y, Maher J, Pak YA, Pedersen JM, Polli JW, Rodrigues AD, Watkins PB, Yang K, Yucha RW, International Transporter Consortium. 2018. Can bile salt export pump inhibition testing in drug discovery and development reduce liver injury risk? An International Transporter Consortium perspective. Clin Pharmacol Ther 104:916–932. https://doi.org/10.1002/cpt.1222.
29. Bam RA, Yant SR, Cihlar T. 2014. Tenofovir alafenamide is not a substrate for renal organic anion transporters (OATs) and does not exhibit OAT-dependent cytotoxicity. Antivir Ther 19:687–692. https://doi.org/10.3851/IMP2770.
30. GlaxoSmithKline/ViiV Healthcare. 2018. Epivir (lamivudine). https://www.gsksource.com/pharma/content/dam/GlaxoSmithKline/US/en/Prescribing_Information/Epivir/pdf/EPIVIR-PI-PIL.PDF.
31. Sjögren E, Lennernäs H, Andersson TB, Gråsjö J, Bredberg U. 2009. The multiple depletion curves method provides accurate estimates of intrinsic clearance (CLint), maximum velocity of the metabolic reaction (Vmax), and Michaelis constant (Km): accuracy and robustness evaluated through experimental data and Monte Carlo simulations. Drug Metab Dispos 37:47–58. https://doi.org/10.1124/dmd.108.021477.
32. Rane A, Wilkinson GR, Shand DG. 1977. Prediction of hepatic extraction ratio from in vitro measurement of intrinsic clearance. J Pharmacol Exp Ther 200:420–424.
33. Chu X, Cai X, Cui D, Tang C, Ghosal A, Chan G, Green MD, Kuo Y, Liang Y, Maciolek CM, Palamanda J, Evers R, Prueksaritanont T. 2013. In vitro assessment of drug-drug interaction potential of boceprevir associated with drug metabolizing enzymes and transporters. Drug Metab Dispos 41:668–681. https://doi.org/10.1124/dmd.112.049668.
34. Chu XY, Bleasby K, Yabut J, Cai X, Chan GH, Hafey MJ, Xu S, Bergman AJ, Braun MP, Dean DC, Evers R. 2007. Transport of the dipeptidyl peptidase-4 inhibitor sitagliptin by human organic anion transporter 3, organic anion transporting polypeptide 4C1, and multidrug resistance P-glycoprotein. J Pharmacol Exp Ther 321:673–683. https://doi.org/10.1124/jpet.106.116517.
35. Monteagudo E, Fonsi M, Chu X, Bleasby K, Evers R, Pucci V, Orsale MV, Cianetti S, Ferrara M, Harper S, Laufer R, Rowley M, Summa V. 2010. The metabolism and disposition of a potent inhibitor of hepatitis C virus NS3/4A protease. Xenobiotica 40:826–839. https://doi.org/10.3109/00498254.2010.519061.
36. Rizk ML, Houle R, Chan GH, Hafey M, Rhee EG, Chu X. 2014. Raltegravir has a low propensity to cause clinical drug interactions through inhibition of major drug transporters: an in vitro evaluation. Antimicrob Agents Chemother 58:1294–1301. https://doi.org/10.1128/AAC.02049-13.
37. Fahmi OA, Shebley M, Palamanda J, Sinz MW, Ramsden D, Einolf HJ, Chen L, Wang H. 2016. Evaluation of CYP2B6 induction and prediction of clinical drug-drug interactions: considerations from the IQ Consortium Induction Working Group—an industry perspective. Drug Metab Dispos 44:1720–1730. https://doi.org/10.1124/dmd.116.071076.
38. Yee KL, Ouerdani A, Claussen A, de Greef R, Wenning L. 2019. Population pharmacokinetics of doravirine and exposure-response in individuals with HIV-1. Antimicrob Agents Chemother 63:e02502-18. https://doi.org/10.1128/AAC.02502-18.